Published in final edited form as:
Biochemistry. 2007 March 20; 46(11): 3366–3377.

The Reducing Activity of Glutaredoxin 3 Towards Cytoplasmic Substrate Proteins is Restricted by Methionine 43

Amir Porat[1,‡], **Christopher Horst Lillig**[2], **Catrine Johansson**[2,#], **Aristi Potamitou Fernandes**[2,§], **Lennart Nilsson**[3], **Arne Holmgren**[2], and **Jon Beckwith**[1,¶,*]

1*Department of Microbiology and Molecular Genetics Harvard Medical School 200 Longwood Avenue Boston, MA 02115 USA*

2*Medical Nobel Institute for Biochemistry, Department of Medical Biochemistry and Biophysics, Karolinska Institute, S171 77 Stockholm Sweden*

3*Karolinska Institutet Department of Biosciences and Nutrition SE-141 57 Huddinge, Stockholm Sweden*

Abstract

The reducing proteins glutaredoxin 3 (Grx3) and glutaredoxin 1 (Grx1) are structurally similar but exhibit different specificities toward substrates. Grx1 efficiently reduces ribonucleotide reductase and PAPS reductase, while Grx3 reduces these enzymes inefficiently or not at all. We previously described a selection for Grx3 mutants with increased activity toward substrates of Grx1 *in vivo*. Remarkably, we repeatedly isolated mutants with changes in only one of the amino acids of Grx3, methionine 43, converting it to either valine, leucine or isoleucine. In this paper we present additional genetic studies and a biochemical characterization of Grx3-Met43Val, the most efficient mutant. We show that Grx3-Met43Val is able to reduce ribonucleotide reductae and PAPS reductase much more efficiently than the wild-type protein *in vitro*. The altered protein has an increased V_{max} over that of Grx3, nearly the same V_{max} as Grx1 while the K_m remains high. Molecular dynamics simulations suggest that the Met43Val substitution results in changes in properties of the N-terminal cysteine of the active site leading to a considerably lower p*K*a. Furthermore, Grx3-Met43Val shows an 11 mV lower redox potential than the wild-type Grx3. These findings provide biochemical and structural explanations for the increased reductive efficiency of the mutant Grx3.

The proteins comprising the thioredoxin superfamily are found in large numbers in all organisms (1-3). These proteins use the redox chemistry of pairs of cysteines to carry out either reductive or oxidative reactions. The majority of these proteins present the simple basic structure of the thioredoxin fold along with a Cys-x-x-Cys active site. The prototypical member of this family is thioredoxin 1 of *E. coli*, which has a molecular weight of 12 kD. For many other members, the thioredoxin fold may be only one domain of a multi-domain protein or may have inserted into it polypeptide sequences that add to the functional activity of the protein (4-6).

‡Current address: ProSci-Inc., 12170 Flint Pl., Poway, CA 92064
#Current address: Biotechnology, The Structural Genomics Consortium, University of Oxford, Botnar Research Centre, Oxford OX3 7LD, The United Kingdom
§Current address: Division of Pathology, Department of Laboratory Medicine, Karolinska Institutet, Karolinska University Hospital in Huddinge, SE 141 86 Stockholm, Sweden
¶To whom correspondence should be addressed: Dept. of Microbiology and Molecular Genetics, Harvard Medical School, 200 Longwood Ave., Boston, MA, U.S.A. Tel.: 617-432-1920; Fax: 617-738-7664; E-mail: jbeckwith@hms.harvard.edu
*Corresponding author. Mailing address: Jon Beckwith, Department of Microbiology and Molecular Genetics, Harvard Medical School, 200 Longwood Avenue, Boston, MA, 02115, USA. Phone: (1-617) 432 1920. Fax: (1-617) 738 7664. E-mail: jbeckwith@hms.harvard.edu

In *E. coli*, the basic thioredoxin structure is found in a number of cytoplasmic proteins that perform reductive reactions. These include thioredoxins 1 and 2, glutaredoxins 1, 2, 3, and 4 and NrdH (7-10). Excluding glutaredoxin 2, which has some features distinguishing it from the other proteins and has a molecular weight of 24.3 kD, these proteins range in molecular weight from 9.1 kD to 15.5 kD (2,8). While some overlap in substrate specificity for these proteins has been observed, these proteins still can vary significantly in their specificity despite their quite similar three-dimensional structures and the short length of their polypeptide chains. The most important of these substrates for aerobic growth of *E. coli* is ribonucleotide reductase, the enzyme which generates deoxyribonucleotides essential for DNA replication. This enzyme, product of the *nrdA,B* genes, uses redox active cysteines for its reductive reaction and must be regenerated as an active enzyme by thioredoxin family members. Specifically, expression of any one of the three proteins, thioredoxin 1, thioredoxin 2 (when overexpressed) or glutaredoxin 1, is sufficient for regeneration of active ribonucleotide reductase (8,11-14). A mutant lacking all three proteins is unable to grow and we have shown that ribonucleotide reductase is the only essential enzyme that requires the presence of at least one of these thioredoxin family members (15).

We are interested in determining which features of the thioredoxin superfamily members are responsible for their differing specificities. Clearly for the glutaredoxins, a glutathione-binding site allows these proteins to receive their electrons from glutathione while thioredoxins are reduced by thioredoxin reductase. But this structural difference is unlikely to explain much or any of the variation in substrate specificity. Are the differences due to differing affinities between enzymes and substrates, to variations in redox potential among these proteins, to differences in the catalytic properties of their active site, or are there other unanticipated features of the proteins involved?

To answer these questions, we have begun to analyze the differences in specificity between two of the *E. coli* thioredoxin family members, glutaredoxins 1 and 3. Glutaredoxin 3 is the most abundant of the three glutaredoxins, although, remarkably, the substrate of this protein has not yet been identified. Glutaredoxin 3 does not reduce ribonucleotide reductase efficiently and, therefore, by itself, does not generate enough activity of the enzyme *in vivo* to allow growth (2,7). Glutaredoxin 2 is even less effective in this reductive reaction (7,16). Thus, a mutant strain we have constructed (RO36), which is missing thioredoxins 1 and 2 and glutaredoxin 1, is unable to grow on rich or minimal media (15). In addition to ribonucleotide reductase, these reductants are required for the regeneration of active phosphoadenylylsulfate (PAPS) reductase, an enzyme involved in sulfur assimilation and, thus the biosynthesis of cysteine (17). Our approach has been to use the properties of RO36 to isolate mutants of glutaredoxin 3, encoded by the *grxC* gene, that are able to reduce ribonucleotide reductase sufficiently to allow growth of *E. coli* on rich media (15). (RO36 also contains a null mutation in *nrdH*, which encodes a thioredoxin-like molecule capable of suppressing the growth defect when overproduced. (9)). In this way, we repeatedly obtained mutational alterations of *grxC* that affected only one amino acid of glutaredoxin 3, Met43, and changed it to either valine, leucine, or isoleucine. We also showed that these *grxC* mutations restore reduction of PAPS reductase, indicated by the ability of the cells to grow on minimal medium in the absence of cysteine.

The three-dimensional structures of *E. coli* glutaredoxins 1 and 3 are quite similar (18-21). Superposition of the backbone atoms of 50 amino acids throughout the proteins gives a root-mean-square deviation of 1.78Å signifying strong structural similarity. The two proteins share 33% amino acid sequence identity and contain the identical redox active site, Cys11-Pro12-Tyr13-Cys14, located at the beginning of α-helix 1 (Figure 1)(3,22). The structures of both proteins consist of the core thioredoxin-fold, the N-terminal β1, α1, β2 motif and the C-terminal β3, β4, and α3 motif. The two motifs are connected by the loop that contains α2 (Figure 1) (3). Previous reports assigned redox potentials of -198 and -233mV for glutaredoxin 3 and

glutaredoxin 1 respectively, indicating that glutaredoxin 1 is considerably more reducing than glutaredoxin 3 (23). One possible explanation for the increased activity of the glutaredoxin 3 mutants is that the amino acid substitutions have altered the redox potential of the protein or the reactivity of their active site cysteines so the protein behaves more like glutaredoxin 1. If that were the case, one might expect that Met43 would lie close to the active site of the protein. However, this residue is found some distance from the redox active site, located in the middle of α-helix 2, at a position equivalent to that of leucine 48 in glutaredoxin 1 (Figure 1). Leucine 48 is located only 2 positions downstream to residues of the binding site for RNR, which directs it to a disulfide between Cys754 and Cys759 located in the C-terminus of the R1 subunit of RNR. This proximity raised the possibility that the increased activity of the mutants resulted from an improved affinity for RNR.

In this paper, we describe biochemical characterization and molecular dynamics simulations of the strongest of the mutant proteins, Met43Val. We also present further genetic selections for altered specificity mutants of Grx3. Our biochemical and molecular dynamics studies when compared with the wild-type Grx3 protein reveal a significant increase in the V_{max} of the mutant protein towards its substrates, a slightly reduced redox potential, a decreased p*K*a of the amino-terminal cysteine of the active site, and an unchanged K_m for substrate. These results, along with potential structural changes in the protein, are used to explain the increased efficiency of Grx3Met43Val.

EXPERIMENTAL PROCEDURES

Strains, Plasmids and Media

Escherichia coli (*E. coli*) cells were grown in NZ medium (24) at 37°C with the appropriate antibiotics. Dithiothreitol (DTT), glutathione (GSH), NADPH, ATP, BSA, glucose 6-phosphate (G6P), glucose 6-phosphate dehydrogenase (G6PD), ATP sulfurylase and inorganic pyrophosphatase were from Sigma. Strains and plasmids used in this work are listed in Table 1. The wild-type *grxC* gene and three *grxC*mutant genes, originally on the pR01 plasmid were subcloned into pQE30 (Table 1). The primers Grx3-Sph1 (5′ - ACATGCATGCCATATGGCCAATGTTGAAATC - 3′) and Grx3-HindIII (5′ - CCCAAGCTTGGATCCTCATTTCAGCAGCGG - 3′) were designed to generate an Sph1 site at the 5′ end and HindIII site at the 3′ end on the different *grxC* genes by PCR. The PCR fragments were then digested with Sph1 and HindIII endonucleases (New England Biolabs) and cloned into pQE30 plasmid digested with the same endonucleases, downstream and in frame with the His_6 epitope. The ligated product plasmids were transformed into *E. coli* DH5 α and plasmid DNA was prepared (Qiagen miniprep DNA kit). All pQE30 plasmids harboring the *grxC*variants were confirmed by PCR using the primers pQE30_FOR (5′ - GCTTTGTGAGCGGATAAC - 3′) and pQE30_REV (5′-AACCGAGCGTTCTGAACA - 3′)

Protein Expression and Purification

E. Coli Grx1 and Trx1 Pro34His mutant proteins were available in the Holmgren laboratory (22). To overexpress His_6-tagged wild-type Grx3 and the Grx3 mutant proteins, the pQE30 plasmids harboring the different *grxC* variants were transformed into *E. coli* JM109 (Stratagene). JM109 transformants were grown in 1 liter NZ medium at 37°C containing Amp (100 μg/ml) to an $O.D._{600} \sim 0.7$ and expression was induced for 4 - 6 hours by addition of 1mM isopropyl-β-D-thiogalactopyranoside (IPTG). The cells were then harvested by centrifugation at 4000 X g for 10 minutes at 4°C and cell pellets stored over night at -20°C. Each cell pellet derived from 1 liter of culture was dissolved in 30 ml of lysis buffer (50 mM Tris-Cl pH 7.4, 50 mM KCl, 10% glycerol, 20 mM Imidazole, 1 mM phenyl methyl sulfonyl fluoride (PMSF) (Sigma) and EDTA-free Protease Inhibitor Cocktail (Roche). The cells were lysed using a French press (20 psi). Cell lysates were centrifuged at 120,000 X g for 1 hour at

4°C. The supernatant was loaded on a 5 ml Ni-NTA chelating column (Amersham Biosciences) using ÄKTA liquid chromatography system (Amersham Biosciences). The column was washed with buffer A (50 mM Tris-Cl pH 7.4, 50 mM KCl, 10% glycerol, 20 mM Imidazole) and proteins were eluted using a 40 ml gradient of imidazole from 20 mM to 500 mM with buffer B (50 mM Tris-Cl pH 7.4, 50 mM KCl, 10% glycerol, 500 mM Imidazole). Typically, all glutaredoxin 3 variants eluted at about 160 mM imidazole and high homogeneity purified proteins (~99%) were confirmed by 15% SDS-PAGE. The His $_6$-Grx3 proteins were purified on separate columns to ensure that the different variants Grx3 were not mixed. Protein concentration was determined from the absorbance at 280 nm using the molar extinction coefficient 12500 M^{-1} cm^{-1} for Grx1 and 4200 M^{-1} cm^{-1} for Grx3 and Grx3Met43V. The proteins were frozen in liquid nitrogen and stored at -80°C until use. *E. coli* ribonucleotide reductase as a 1:1 mixture of R1 and R2 was a generous gift from Prof. Britt-Marie Sjöberg Department of Molecular Biology, University of Stockholm and treated as described previously (11,12).

Glutaredoxin Activities in the Coupled Reaction with Ribonucleotide Reductase and Determination of Kinetic Constants

In this assay the formation of dCDP from CDP, a reaction catalyzed by ribonucleotide reductase, is measured as described previously (11,12). The final concentrations of the reaction mixture components are: 0.5 mM [^{3}H]CDP, 1.3 mM ATP, 11 mM $MgCl_2$, 0.53 mg/ml BSA, 33 mM Hepes pH7.5, 1.6 mg/ml NADPH, 2.5 μg/ml yeast glutathione reductase (GR), 5 mM glutathione (GSH), 10 mM glucose 6-phosphate (G6P) and 2.5 μg/ml glucose 6-phosphate dehydrogenase (G6PD). G6P and G6PD were used as an NADPH regenerating system. Glutaredoxin 1 and 3 and glutaredoxin 3 Met43Val were reduced with 5 mM dithiothreitol (DTT) for 30 minutes on ice and desalted on a Sephadex G-25 column (PD10 column Amersham Biosciences) with 50 mM Tris-Cl pH7.5 and 5 mM EDTA and immediately used. Increasing amounts (0.1-30 μM) of the reduced glutaredoxins were added to the reaction mixture and the reaction was started by adding 2 μg of *E. coli* ribonucleotide reductase to a final volume of 120 μl resulting in a final concentration of 0.12 μM. After incubation for 30 minutes at 37°C, the reaction was stopped by addition of 0.5 ml of 1 M perchloric acid (PCA). The reaction samples were boiled for 10 minutes after the addition of 5 mg/ml dCMP and cooled on ice for 10 minutes. The pH was adjusted to 7.0 by 4 M KOH and 0.2 M acetic acid using phenol red as pH indicator. The amount of [^{3}H]dCDP formed was determined after hydrolysis to [^{3}H] dCMP by chromatography on Dowex-50 columns (6 ml bed volume) with 55 ml and 25 ml of 0.2 M acetic acid respectively. The activity in μU was determined as described (25).

In our hands, using the published protocol, neither glutaredoxin 1 nor the Met43Val mutant protein were able to reach saturation in reducing ribonucleotide reductase, making it impossible to determine the kinetic constants. By decreasing 3-fold the amount of ribonucleotide reductase in the assay (from 6 μg to 2 μg) we obtained saturation curves for the Met43Val mutant and for the wild-type glutaredoxins 1 and 3 (Figure 2A). The kinetic constants were determined from two sets of experiments assuming Michaelis-Menten kinetics. Grace software version 5.1.16 (http://plasma-gate.weizmann.ac.il/Grace/) was used to calculate the kinetic constants employing a non-linear regression analysis with K_m and V_{max} as the two variables in the Michaelis-Menten equation.

Glutaredoxin Activities in the Coupled Reaction with 3′phosphoadenylylsulfate (PAPS) Reductase and Determination of Kinetic Constants

PAPS reductase was expressed and purified as described (26). PAPS reductase activity was measured following the reduction of NADPH in a coupled assay with yeast glutathione reductase at 30°C. The assay mixture (550 μl) contained 100 mM Tris-HCl pH 8.0, 200 μM

NADPH, 5.75 μg glutathione reductase, 2 mM reduced glutathione and glutaredoxins as indicated. NADPH consumption was recorded by following the decrease in absorbance at 340 nm in a dual beam spectrophotometer (UV-2100, Shimadzu). Both cuvettes contained the assay mixture and the reaction was initiated by the addition of 0.25 - 3 μg of PAPS reductase to the test cuvette. PAPS was synthesized enzymatically as described by Schriek and Schwenn (27) using ATP sulfurylase, inorganic pyrophosphatase, pyruvate kinase (Roche) and APS kinase from *Arabidopsis thaliana* purified according to Lillig *et al.* 2001 (28). The kinetic constants were determined from two sets of data using nonlinear regression of the datasets assuming Michaelis-Menten kinetics.

Comments on the two enzyme assays—The kinetic constants were calculated employing non-linear regression analysis with K_m and V_{max} as variables assuming Michaelis-Menten kinetics. The regression coefficients obtained from these calculations were in the range of 0.96 to 0.99, indicating that the data points followed Michelis-Menten kinetics. Three or more independent datasets were obtained and the standard deviation of the kinetic constants was usually between 5 and 20 %.

Determination of Protein Equilibrium Constants and Redox Potentials for Grx3 and Grx3 Met43Val

The redox potential for *E. coli* Grx3 and Grx3 Met43Val was determined using direct protein-protein redox equilibria essentially as described by Åslund *et al.* 1997 (23). In this method two redox active proteins are mixed where initially one is fully oxidized and the other is fully reduced. Equilibrium reactions (100 μl) were performed by incubating equal concentrations (50 μM) of either His_6-tagged Grx3 or His_6-tagged Grx3 Met43Val with either Grx1 or Trx1 Pro34His in degassed and N_2-purged solutions of 100 mM potassium phosphate pH 7.0 and 1 mM EDTA. The reaction was initiated by adding one of the proteins in the reduced state and the other in the oxidized state. The reduced protein was prepared immediately before use by incubation with 5 mM DTT at room temperature for 1 hour followed by desalting on a Sephadex G-25 column (NAP-5, Amersham Biosciences). After different time points (between 6 and 20 hours) under N_2(g), the reaction were quenched by addition of 1M phosphoric acid to a final pH of 2.5. The reduced and oxidized forms of the proteins were analyzed by reverse phase HPLC (Pharmacia SMART micropurification system) on a C_8 column (2.1 mm × 10 cm) using a linear gradient of 22% to 55% (v/v) acetonitrile, 0.1% (v/v) trifluoroacetic acid (TFA) in 130 minutes at a flow rate of 50 μl/min. Proteins eluted from the column were monitored at 214 nm and the peak identification determined in separate runs using only the oxidized and the reduced protein. The redox potentials of His_6-tagged Grx3 and His_6-tagged Grx3 Met43Val were calculated using the Nernst equation and the integrated peak areas of the oxidized and reduced form of the proteins in the chromatogram.

Molecular Dynamics Protocols and p*K*a *Calculation*

A structural model for the Grx3 M43V mutant was constructed from the Grx3 wt structure with Cys11 in the thiolate form (19) by deleting S^{δ} and the C^{ε} methyl group. One of the valine side chain methyl carbons was given the position of the methionine C^{γ} and then the second methyl carbon of Val43 could be unequivocally placed. Missing hydrogens were added in standard positions. This model was solvated with TIP3P water molecules (29) and one Cl^- ion was added at a random position to make the system electrically neutral. Constant pressure (30) and temperature simulations were then performed at 1 atm. and 298K using periodic boundary conditions in a rhombic dodecahedron cut out of a cube with edge length 52Å. Non-bonded energies and forces were smoothly shifted to zero at a cutoff of 12Å, with the non-bond list generated to 14Å and updated as soon as any atom had moved > 1Å since the last list-update. This is a cutoff method that has been shown to work well even for highly charged species, such as nucleic acids. (31,32) Bonds involving hydrogens were constrained using the

SHAKE algorithm (33) allowing a 2 fs time step for the numerical integration. Three independent simulations (using different initial velocity assignments) of 16 ns were performed. In each simulation the first 5 ns was considered equilibration, and was not used for data collection, resulting in a total of 33 ns of sampling. Water-water interactions were computed using an efficient table-lookup algorithm (L. Nilsson, manuscript in preparation).

Snapshots taken every 0.1 ns of the trajectory were used in calculating p*K*a values for the Cys11 and Cys14 S^{γ}, using the same protocol as previously published (18,19) for the wild-type Grx3 with a finite difference solution of the linearized Poisson-Boltzmann (PB) equation implemented in CHARMM (34,35) at 0.15M ionic strength and with a 2Å ion exclusion layer, using the atomic radii of Nina et al (35), relative dielectric coefficients of 3 and 78 for the protein and water, respectively, and a reference value of 8.3 for the p*K*a of a free Cysteine. Only the protein part of the system was included in these calculations, according to standard practice when using continuum descriptions (36).

Hydrogen bonds were defined using a simple distance criterion r(H...A) < 2.4Å (37) for all hydrogen bonds except those involving sulfur atoms when a 3.0Å cutoff was used (19). All calculations were performed with the CHARMM program package (38) using the all-atom parameter set version 22 (39). The recently added correction term for backbone torsions (40) was not included in our setup to allow for a direct comparison with previous studies of the wild type Grx3 (18,19). The correction can however be assumed to be of minor importance for this globular, and quite stable protein, the overall structure of which did not change significantly during the simulations. It can also be noted that the predicted local structure of the Grx3 active site, using this force field and simulation protocol, was verified by NMR (19).

Solvent accessible surface areas (ASA) (41) were calculated using a probe radius of 1.4Å.

RESULTS

An additional selection for glutaredoxin 3 mutants

We have previously described a genetic selection for glutaredoxin 3 mutants with enhanced activity towards the glutaredoxin 1 substrate, ribonucleotide reductase (15). The mutations all affected the same amino acid, Met43, chainging it to either leucine, isoleucine or valine. We asked whether we could obtain mutants with different alterations in the specificity of glutaredoxin 3 by selecting for mutants that allowed reduction of PAPS reductase, rather than ribonucleotide reductase. The defect in PAPS reductase results in a requirement for cysteine when the bacteria are grown on minimal media. However, ordinarily a selection for restoration of PAPS reductase activity would not be possible without also selecting for ribonucleotide reductase at the same time, since the latter enzyme is required for growth under all conditions. We have described a strain in which restoration of PAPS reductase activity can be selected for independently of restoration of ribonucleotide reductase activity. Strain RO34 is a derivative of strain RO36 in which a *dnaA* mutation has caused a derepression of ribonucleotide reductase. This derepression overcomes the growth defect on rich media of the multiple glutaredoxin/thioredoxin mutant by allowing sufficient reduction of the overexpressed ribonucleotide reductase by the weak reductant glutaredoxin 3 (15). However, the strain still requires cysteine on minimal media, as this bypassing of one of the strain's requirements has no effect on the lack of reduction of PAPS reductase.

We have carried out error-prone PCR mutagenesis of the *grxC*gene with different AG/CT ratios as described previously (15) and introduced the mutagenized plasmid into strain RO34. This mutagenesis yields approximately one base substitution every 300 base pairs (15). In this case, we carried out 20 separate PCR reactions and isolated five independent mutants in which growth is restored in the absence of cysteine in minimal media from approximately 100,000

transformants. Sequencing shows that the mutations in each of the five strains caused the same substitution in glutaredoxin 3, Met43Val. (All A to G transitions) Thus, alterations in specificity of glutaredoxin 3 towards two different substrates always appear in the same amino acid residue. We further asked, using oligonuceotide-directed mutagenesis, whether substituting an alanine for Met43 might result in improved reductive ability of glutaredoxin 3. This alteration did appear to restore some growth to strain RO36 on rich media, if weakly, but did not restore growth to strain RO34 on minimal media without cysteine. We have not excluded the possibility that the alanine substitution caused instability of the protein explaining its low activity.

The glutaredoxin 3 Met43Val mutant protein reduces ribonucleotide reductase in-vitro

We have purified the wild-type glutaredoxin 3 protein and its mutant variants in order to study their biochemical properties. To this end, the *grxC* gene and the three altered *grxC* genes were cloned into the pQE30 plasmid downstream and in-frame to a His_6 tag. The pQE30 plasmids were introduced into *E. coli* strain JM109 and the resultant strains induced with isopropyl-β-D-thiogalactopyranoside (IPTG). The overexpressed proteins were affinity-purified to near homogeneity on a Nickel chelating column.

To examine the ability of the glutaredoxin 3 variants to reduce ribonucleotide reductase *in vitro*, increasing amounts of the proteins were added to the standard ribonucleotide reductase assay and the conversion of ribonucleotide 5′-diphosphates (CDP) to deoxy-CDP (dCDP) was measured by chromatography. Preliminary experiments indicated that the Met43Val mutant protein significantly enhanced the activity of ribonucleotide reductase whereas glutaredoxin 3 Met43Leu, which *in vivo* was the second strongest reductant of the three Met43 changes, as indicated by colony size on rich media, showed variable results with significant fluctuations in ribonucleotide reductase activity (Data not shown). This mutant showed higher activity than wild type as an electron donor towards ribonucleotide reductase only at low concentrations of 0.25 and 1.0 μM (Data not shown). In repeated independent assays [7] with glutaredoxin 1 or glutaredoxin 3 Met43Val as positive controls, the data points for Met43Leu did not follow Michaelis-Menten kinetics. The kinetic studies with Met43Leu yielded V_{max} activities close to that of wild type glutaredoxin 3, but with considerably high standard deviations. For these reasons, we did not continue studies with this mutant protein, nor with the Met43Ile protein which showed the weakest effects *in vivo* and restricted further studies to the Met43Val protein.

Saturation curves show that the Met43Val mutant protein efficiently reduces ribonucleotide reductase *in vitro*; increasing amounts of the protein significantly stimulate ribonucleotide reductase activity reaching saturation with the mutant protein at 17 μM (Figure 2A). Ribonucleotide reductase activity was stimulated at much lower concentrations when glutaredoxin 1 was used as electron donor (0.85 μM); however, maximal activity was similar to that of glutaredoxin 3 Met43Val (Figure 2A). Consistently, we observed inhibition of the activity at high levels of glutaredoxins, an effect previously seen also with thioredoxin 1 and DTT ((42) and A. Holmgren, unpublished results). This effect may be due to substrate inhibition. The wild-type glutaredoxin 3 showed poor activity toward ribonucleotide reductase, confirming previous findings.

To determine the kinetic constants for these reactions, we used non-linear regression analysis to plot the kinetics (Figure 2B) and to calculate V_{max}'s and K_m's for the three glutaredoxins, assuming Michaelis-Menten kinetics. Glutaredoxin 1 and glutaredoxin 3 Met43Val exhibit similar V_{max} values of 113 +/- 9.0 nmol mg^{-1} min^{-1} and 122 +/- 4.0 nmol mg^{-1} min^{-1} respectively (Figure 2B, Table 2). These values differ sharply from that of wild-type glutaredoxin 3, which shows a V_{max} of only 18 +/- 1.5 nmol mg^{-1} min^{-1}. While the V_{max} of the mutant protein is dramatically increased over that of glutaredoxin 3, its K_m remains essentially the same. The K_m values for glutaredoxin 3 Met43Val and wild-type glutaredoxin 3 protein

are 4.3 +/- 0.8 μM and 3.5 +/- 0.95 μM, respectively while that of glutaredoxin 1 is lower (equal to or less than 0.17 +/- 0.01 μM), close to the previously reported 0.13 μM (Table 2). (The calculated K_m suffers from the inaccuracy involved in using the high enzyme concentration necessary in the ribonucleotide reductase assay.)

From the kinetic parameters (Figure 2B and Table 2), we calculate that the Met43Val mutant protein is 5- to 6-fold more efficient than glutaredoxin 3, but still very inefficient compared to the 23-fold more efficient glutaredoxin 1 (Table 2). These efficiency differences in the catalytic activity between the mutant protein and glutaredoxin 1 are attributable to the 25 times lower K_m of glutaredoxin 1 whereas the efficiency differences between the mutant protein and glutaredoxin 3 are almost exclusively the result of differences in their V_{max}'s (Table 2). Thus, the major kinetic parameter altered in glutaredoxin 3 Met43Val is its increased V_{max} in the reaction with ribonucleotide reductase.

PAPS reductase is reduced in vitro by the glutaredoxin 3 Met43Val mutant protein

The glutaredoxin 3 Met43Val alteration, in addition to restoring growth on rich medium to the multiply mutant strain RO36, also eliminates the cysteine prototrophy of this strain observed on minimal medium (see Introduction). Therefore, we asked whether this mutant protein is able to reduce PAPS reductase *in vitro*. We employed a new assay to measure PAPS reductase activity using as electron sources either glutaredoxin 3 Met43Val, glutaredoxin 3 or glutaredoxin 1. In this assay, the reduction of PAPS to PAP and sulfite by PAPS reductase is measured indirectly by coupling the reaction to the oxidation of NADPH by glutathione reductase. Addition of glutaredoxin 1 to the assay resulted in a rapid increase of PAP and sulfite and after about 2 minutes the reduction of PAPS slowed down because all of the PAPS in the assay was consumed (Figure 3A). Addition of the Met43Val mutant protein to the assay resulted in constant production of PAP and sulfite, although the rate of production was lower than that seen with glutaredoxin 1 as indicated by the milder slope shown in figure 3A. Glutaredoxin 3 was inactive as an electron donor for PAPS reductase (Figure 3A), a result consistent with previous studies that fail to show reduction of PAPS reductase by glutaredoxin 3 *in vivo* (17) and *in vitro* (26).

With the concentration of PAPS near saturation, we assumed Michaelis-Menten kinetics for PAPS reductase to determine the V_{max} and K_m from two sets of data using nonlinear regression analysis (Figure 3B, analysis shown for the mutant only) of the data sets. For glutaredoxin 1 we found a K_m value of 12.7 +/- 0.9 μM and a V_{max} of 4.1 +/- 0.3 μmol mg^{-1} min^{-1} (Table 3). These kinetic constants are similar to the previously reported K_m and V_{max} values of 14.9 μM and 5.1 μmol mg^{-1} min^{-1} respectively (26). The K_m and V_{max} calculated for the altered glutaredoxin 3 were 79.5 +/- 2.3 μM and 3.1 +/- 0.3 μmol mg^{-1} min^{-1}, respectively. These kinetic parameters indicate that the altered glutaredoxin 3 reactivates PAPS reductase because of its V_{max} which is similar to that seen when glutaredoxin 1 is used as a reductant (Table 3). The large difference in the K_m's of the two proteins results in glutaredoxin 1 being 8-fold more efficient as an electron donor for PAPS reductase than the glutaredoxin 3 Met43Val (Table 3)

The altered glutaredoxin 3 (Grx3 Met43Val) is a better reductant than the wild-type protein

An important feature of redox proteins determining their relative abilities to reduce or oxidize substrates is their redox potentials (43). Since glutaredoxin 3 has a higher redox potential than glutaredoxin 1, making it a less effective reductant in general, we considered the possibility that the Met43Val change in glutaredoxin 3 may have decreased its redox potential. The technique most commonly used to determine a protein's redox potential measures equilibrium concentrations of the oxidized and reduced forms of the protein using defined ratios of GSH/GSSG as a redox reference. However, since glutaredoxins already normally interact with glutathione and accumulate significant amounts of GS-Hmixed disulfide intermediates (11,

44), we used the protein-protein redox equilibrium as described in Åslund. *et al 1997* (23). The differences in redox potentials between two proteins can be determined, using the Nernst equation, by measuring the concentrations of their oxidized and reduced forms at equilibrium. The relative amounts of the individual species (reduced and oxidized for each protein) at equilibrium were determined by integration of the peak areas of the chromatogram eluted from the reverse phase HPLC column. To be able to distinguish between fully reduced and oxidized species of the proteins in question, separate runs of reduced and oxidized forms were done to determine the elution profiles (Data not shown).

We first determined the redox potential of N-terminally His_6-tagged glutaredoxin 3 (Grx3) using glutaredoxin 1 (Grx1) as a reference (Figure 4A). We calculated the apparent concentration equilibrium constant, $K'_{1,2}$, for Grx1 and Grx3 to be 24.3 at pH 7.0 (Figure 4A). Thus, by placing this value in the Nernst equation we calculated that Grx3 is 41 mV more oxidizing than Grx1. The 41 mV difference gives a -192 +/- 2 mV redox potential for Grx3, which is 6 mV more oxidizing than the published redox potential for Grx3 of -198 mV. We determined a value for $K'_{1,2} = 10.5$ between Grx1 and the Grx3 Met43Val under the same conditions used for wild-type Grx3 (Figure 4B). Thus, according to our calculations, using the Nernst equation and $K'_{1,2} = 10.5$, the Grx3 mutant protein is 30 mV more oxidizing than Grx1. The 30 mV difference between Grx1 and Grx3 Met43Val yields a redox potential of -203 +/- 2 mV for the mutant. Thus, our results indicate that the Grx3 Met43Val exhibits a redox potential 11 mV lower than that of Grx3 suggesting that the mutant is a better reductant with a redox potential closer to that of Grx1. These redox potential determination experiments were repeated twice. In addition, we determined the redox potential of Grx3 Met43Val by using a thioredoxin 1 mutant, Pro34His (23), as a partner instead of Grx1 (Figure 4C). Trx1-P34H has a redox potential of -235 mV (49) and calculation of protein-protein equilibrium with Grx3-M43V indicate that the Grx3 mutant protein is 31 mV more oxidizing then its partner Trx1 mutant. These results confirm that the Grx3 mutant protein is 11 mV more reducing than wild type Grx3.

The Met43Val mutation significantly lowers the p*Ka of the active site N-terminal Cysteine*

Glutaredoxin 1 and 3 share identical active site motifs, -Cys11-Pro12-Tyr13-Cys14-, at identical positions of their sequences. However, comparison of the active site of the two proteins by molecular dynamics simulations and electrostatic calculations uncovered differences in the structure, dynamics, and electrostatic interactions of these active sites (18). The calculated average values of the N-terminal cysteine p*K*a (pK_a^{11}) in glutaredoxins 1 and 3 is virtually identical and lies around a p*K*a value of ~5.0 (18). Yet, these average values cover subtle differences. Molecular dynamics simulations previously demonstrated that pK_a^{11} in glutaredoxin 1 constantly fluctuates between values of 6.8 and 2.7 (18). These apparent and frequent fluctuations are for the most part the result of intermittent hydrogen bonding between Cys11 S^{γ} and Arg8 N^{ε} and N^{η} that occur on average more than 31% of the time (18). In contrast pK_a^{11} of glutaredoxin 3 does not show frequent fluctuations and the simulations suggest that the hydrogen bond between Cys11 S^{γ} and Lys8 N^{ζ} is formed intermittently less than 10% of the time (18). The p*K*a of thiols in the active site is key to the reactivity of its sulfur and low p*K*a of the N-terminal thiol affects its nucleophilic power and the leaving group ability of the C-terminal thiolate (45,46).

To examine whether the active site of glutaredoxin 3 Met43Val takes on structural features similar to those observed in glutaredoxin 1, we initiated molecular dynamics simulation experiments on glutaredoxin 3 Met43Val. We analyzed the results with regard to the previously reported data on wild type glutaredoxin 3 (18). We find no large structural changes in the mutant, and overall it behaves very similarly to the wild type in the simulations. However the calculated p*K*a value for Cys11 from three independent simulations is significantly lower in

the mutant (3.8, estimated error ~0.5 units) than in the wild type (4.9) (Figure 5). For Cys14 the p*K*a is also lower in Met43Val, but not by as much (13.6 *vs* 14.4). The distribution of p*K*a values for Cys11 in Met43Val is not only shifted to lower values compared to the wild type, but it is also broader, in particular towards the low p*K*a range, than in the wild type (Figure 5).

The lowered pKa^{11} of glutaredoxin 3 Met43Val raised the possibility that Lys8 might play a role in this mutant protein via interactions such as a hydrogen bond between $S^{\gamma}{}_{11}$ to $N^{\zeta}{}_{8}$. Previous simulations with wild-type glutaredoxin 3 were somewhat ambiguous on this point because the simulations were carried out for a short period of time (19). Extended simulations reported hydrogen bond formation ($S^{\gamma}{}_{11}\cdots\cdots N^{\zeta}{}_{8}$) less then 10% of the time. The dynamic simulations in the Met43Val mutant indicate that the Lys8 side chain spends more time in the vicinity of Cys11 S^{γ} than it does in the wild type simulations (Table 4). Lys8 and Cys11 are within hydrogen bonding distance 19% of the time in the Met43Val (average distance 5.9Å) and 6% of the time in the wild type (average distance 6.9Å) (Tables 4 and 5). On average the total number of hydrogen bonds to Cys11 S^{γ} is greater in the Met43Val (4.2) than in the wild type (3.8). The correlation coefficient between the p*K*a of Cys11 and the number of protei-n Cys11 S^{γ} hydrogen bonds formed during the analyzed 33 ns of simulation was -0.58 (more hydrogen bonds result in a lower p*K*a), indicating that although these hydrogen bonds do play an important role for this p*K*a, there are also other factors that contribute.

In addition to the previously described (19) hydrogen bonds to Cys11 from Cys14 S^{γ} and the backbone amides of Tyr13 and Cys14, there is also a very stable water molecule bridging Cys11 S^{γ} and Val52 O (Figure 6). Although this water molecule is also present in the wild type simulations, the average Cys11 S^{γ} to Val52 O distance is slightly shorter in Met43Val (Table 5, Figure 7), which may make for an energetically more favorable contact in the mutant. There is also a greater possibility of having a water bridge between Cys11 S^{γ} and Lys8 in Met43Val than in the wild type (34% vs. 16%) (Table 4). Not only is the average distance shorter in the mutant, the Cys11 to Lys8/Val52 distance distributions (Figure 7) are slightly narrower in the mutant, suggesting that these enhanced hydrogen bonds in the mutant drive the Cys11 S^{γ} to a thiolate form. The Met43Val mutation may influence these interactions since the side chain of residue 43 packs directly onto the hydrophobic side chain of Val52 (Figure 6). These results suggest additional contributions that favor a lower pKa^{11} in the mutant and together with the improved (higher frequency) hydrogen bond profile with Lys8 may explain the reduction in the p*K*a of the Cys11 observed in the simulations for glutaredoxin 3 Met43Val. Neither the fluctuations of atoms around their average positions, nor the distances Cys11 - Met43 and Cys11 - Val43 exhibit any differences between the wild-type and mutant Grx3 proteins.

DISCUSSION

In this paper, we describe studies directed towards understanding the differing specificities of two members of the thioredoxin superfamily. The protein glutaredoxin 1 shows high reductive activity towards the substrates ribonucleotide reductase and PAPS reductase. In contrast, the protein glutaredoxin 3, a homologue of glutaredoxin 1, is incapable of efficiently reducing ribonucleotide reductase and PAPS reductase both *in vivo* and *in vitro*. We present the biochemical characterization of a mutant Met43Val version of glutaredoxin 3, which shows a substantial increase in activity towards these substrates. This change is manifested phenotypically in the ability of the cells to make sufficient deoxyribonucleotides for growth on rich medium and in the elimination of the cysteine auxotrophy seen when PAPS reductase is not regenerated as an active enzyme.

While, in addition to glutaredoxin 1, thioredoxins 1 and 2 are capable of reducing ribonucleotide reductase, we have focused our biochemical studies on a comparison between

the properties of glutaredoxins 1 and 3, since they exhibit both strong sequence and structural homologies. We show that the single amino acid change Met43Val in glutaredoxin 3 alters three of the four properties of the protein that we have assessed. First, the Met43Val change greatly increased the V_{max} of the mutant enzyme with ribonucleotide reductase, elevating it to practically the same level as glutaredoxin 1, thus increasing the *kcat* by ~7-fold. The altered protein also exhibited a V_{max} for PAPS reductase comparable to that measured for glutaredoxin 1. Wild-type glutaredoxin 3 is inactive in the reduction of PAPS reductase and thus, a V_{max} is not measurable.

Second, the Met43Val change shifted the redox potential of glutaredoxin 3 to a lower value making it potentially a more effective electron donor. We measured a significant 11 mV decrease in redox potential (-203 mV) from that observed with the wild-type glutaredoxin 3 (-192 mV), moving the redox potential of the mutant protein towards that of glutaredoxin 1 (-233 mV). Our measurements for glutaredoxin 3 suggest that the wild-type protein is 6 mV more oxidizing than previously reported. The difference might be explained by the fact that the previous study determined the redox potential for a Grx3-Cys65Tyr mutant protein in which cysteine 65, a third cysteine not part of the redox active site, was eliminated. Alternatively, the differences could be due to the difficulties in fully separating the oxidized and the reduced Grx3 in the present study. Notably, the redox potential of wild-type Grx3 was recently determined to be -194 mV, consistent with our findings (50). Third, molecular dynamics simulations indicate a significantly lowered p*K*a of the N-terminal active site cysteine of the Met43Val protein. This changed p*K*a would result in an increase in the thiolate anion form of this cysteine, which would be more effective in attacking a disulfide bond in a protein substrate. In contrast to the first three properties of the Grx3Met43Val protein measured, the fourth property, its K_m for ribonucleotide reductase remains high and essentially unchanged from that of the wild-type glutaredoxin 3 and thus is much higher (~20-fold) than that of glutaredoxin 1. The measured K_m of glutaredoxin 3 Met43Val for PAPS reductase is also 6-fold higher than that measured for glutaredoxin 1.

We had previously suggested that the altered glutaredoxin 3 might have increased affinity for RNR due to alteration of the structure of the binding site. This hypothesis stems from the notion that Leu48 in glutaredoxin 1, the equivalent residue to Met43 resides close to the RNR binding site (15,43). However, from results presented here, the increased efficiency of the mutant protein cannot be attributed to increased affinities for substrates, as the $K_{m's}$ haves not been altered by the Met43Val change. Rather, the combination of the reduced p*K*a and the lowered redox potential of the protein compared to the wild-type Grx3 could make the protein more effective at attacking disulfide bonds and make the reductive reaction more favored.

The properties of the Grx3Met43Val mutant protein described in this paper provide potential explanations for structural features of the altered protein that are responsible for its increased reductive enzymatic efficiency with substrate proteins. Important to this discussion is the finding that only alterations of Met43 were obtained in repeated selections, despite the fact that different approaches were used to obtain glutaredoxin 3 mutants with enhanced reduction of ribonucleotide reductase and PAPS reductase. These results indicate that the presence of the methionine at position 43 of the protein confers significant restrictions on the activity of this enzyme towards these substrates. Relief of these constrictions without alteration of affinity for substrates could explain the increased V_{max} of the Grx3Met43Val protein.

We suggest two ways in which the Grx3Met43Val change could relieve constrictions on activity towards substrates. First, the increased V_{max} may result from the increased reactivity of the cysteine 11 of the active site predicted by the molecular dynamics simulations. According to this analysis, the Grx3Met43Val substitution has altered interactions within the protein such that Lys8 is more likely to be forming hydrogen bonds with Cys11 and a water molecule is

more likely to bridge between Cys11 and Val52, thus influencing Cys11's activity in attacking disulfide bonds. Based on these simulations, we suggest that the large methionine residue via its interactions with other residues is restricting the Lys8/Cys11 interaction and the water molecule bridging Cys11-Val52. The substitution of the smaller residues in the mutant proteins, Met43Val, Met43Leu and Met43Ile, reduces this restriction, improving the reductive ability of the protein. Strikingly analogous restrictive effects of larger versus shorter aliphatic residues have been observed in other systems. For instance, the single-channel ion conductance in the anthrax toxin pore progressively increased when the wild-type amino acid phenylalanine 427, which lines the heptameric pore, was changed to the smaller aliphatic residues, leucine, isoleucine and valine (in that order) (47). When methionine was substituted for phenylalanine, the conductance was comparable to the wild-type (J. Collier, personal communication).

A second explanation derives from comparisons of the very similar structures of glutaredoxins 1 and 3. We note that in the upper part of the molecules as shown in Figure 1, glutaredoxin 1 appears to exhibit a more 'open' structure and clearly displays a dynamic plasticity that may allow it to adapt to a number of different disulfide substrates (48). In this portion of the structure, the leucine 48 of glutaredoxin 1 is in the same relative position as methionine 43 of glutaredoxin 3. Again, the substitutions of smaller aliphatic residues at this position may make the active site more accessible to substrates

Examination of the structures also shows that leucine 48 of glutaredoxin 1 is at a greater distance from the active site cysteines than is methionine 43 of glutaredoxin 3 (Figure 1). We asked whether we could mimic the proposed restrictive effects of Met43 in glutaredoxin 3 by mutationally replacing Leu48 of glutaredoxin 1 with methionine. However, we saw no observable effect on the activity of Grx1Leu48Met *in vivo* (Porat and Beckwith, unpublished results). This negative result may be due to other features of glutaredoxin 1 or to our having expressed levels of the protein high enough to mask any defects.

We also point out that the substitutions Met43Leu and Met43Ile, which introduce amino acids with longer or more bulky side chains than valine, give weaker *in vivo* phenotypes and, with Met43Leu, a significantly weaker improvement in kinetic constants *in vitro*. This finding is consistent with the proposal that the longer side-chain amino acids are more likely to restrict the activity of the enzyme. On the other hand, the change of Met43 to the even shorter alanine is less effective at improving the reductive ability of the protein as assessed by its weak effect on phenotype. Its weaker activity may be due to the rather drastic change of the very long methionine to the short alanine, thus causing other effects on the structure of the protein (or effects on *in vivo* instability).

Despite the increased activity of glutaredoxin 3 caused by the Met43Val change, glutaredoxin 1 is still a much better reductant than the Grx3Met43Val protein for the substrates examined, exhibiting a 23-fold higher catalytic ability, while the mutant protein itself is 5- to 6-fold more efficient then glutaredoxin 3 (Table 2). Based on our previous results, it was not surprising to see that the relatively inefficient mutant Grx3Met43Val could restore reduction of ribonucleotide reductase sufficient for growth. We had shown that, *in vivo*, even the 130-fold lower catalytic ability of wild-type glutaredoxin 3 compared to glutaredoxin 1 can suffice for the reduction of ribonucleotide reductase when the latter enzyme is greatly overexpressed (15).

We note that while the measured K_m of 0.17 μM of glutaredoxin 1 for ribonucleotide reductase presented here is very similar to that found in earlier studies, the K_m value we have obtained for glutaredoxin 3 (3.5 μM) is significantly higher than the published K_m of 0.35 μM (7). The older measurements were carried out with extracts, not pure proteins. Furthermore, the K_m was measured previously by plotting a linear curve of 1/V as a function of 1/[S] where V is the

reaction rate and [S] is the initial substrate concentration. This linear regression analysis is sensitive to errors at low substrate concentrations as minor fluctuations of the reaction rates drastically change the linear slope. To eliminate this problem, we used an algorithm for non-linear regression analysis. This analysis better represents the saturation curve of enzyme activity as a function of substrate concentration. While our calculations of kinetic parameters are based on relatively few data points, the statistics (standard deviations and correlation coefficients) shown in Tables 2 and 3 indicate that the values obtained are significant. Furthermore, many mathematical models, including that used here, permit such calculations without measurements made with the substrate near saturation.

The finding that repeated selections for mutations of *grxC*that allow reduction of ribonucleotide reductase or independently reduction of PAPS reductase have yielded only alterations of Met43 of glutaredoxin 3 suggests that there may be strong structural constraints on the ability of the protein to interact with glutaredoxin 1 substrates, constraints that may only be relieved by alterations of this residue. These structural constraints are explained in part by the additional C-terminus helix turn that is tightly packed to the core of the protein and thereby increases the "stiffness" of the fold and by the shorter loop that connects α1 to β2 and does not contain two Gly residues as in glutaredoxin 1 (48). The restriction to only Met43 alterations suggests that further use of this genetic approach may not yield any other alterations and not assist in additional genetic analysis of the glutaredoxin 1/glutaredoxin 3 differences. Future studies, therefore, will be directed toward isolating new classes of *grxC*mutants by seeking enhanced activity of the Met43Val version of the protein. With the suggested improved active site or access to substrates of Grx3Met43Val, other classes of mutations altering substrate affinity or more drastic redox potential changes may appear in such genetic selections.

Acknowledgments

We thank Rolf Eliasson for purification and help with assays of ribonucleotide reductase and Anne-Gaelle Planson for comments on the manuscript.

This work was supported by National Institutes of Health Grant GM-41883 from the National Institute of General Medical Sciences (to J.B.), grants from the Swedish Research Council Medicine (3529) and the Swedish Cancer Society (961) (to A. H.), from the Swedish Research Council (to L.N.), and funds from the Karolinska Institute and the Wenner-Gren Foundation.

Abbreviations

DTT, Dithiothreitol; Grx3, Glutaredoxin 3; RNR, Ribonucleotide reductase; PAPS, phosphoadenosine-5-phosphosulfate.

REFERENCES

1. Holmgren A. Thioredoxin and glutaredoxin systems. J Biol Chem 1989;264:13963–13966. [PubMed: 2668278]
2. Fernandes AP, Holmgren A. Glutaredoxins: glutathione-dependent redox enzymes with functions far beyond a simple thioredoxin backup system. Antioxid Redox Signal 2004;6:63–74. [PubMed: 14713336]
3. Martin JL. Thioredoxin--a fold for all reasons. Structure 1995;3:245–250. [PubMed: 7788290]
4. Bardwell JC, McGovern K, Beckwith J. Identification of a protein required for disulfide bond formation in vivo. Cell 1991;67:581–589. [PubMed: 1934062]
5. Kim JH, Kim SJ, Jeong DG, Son JH, Ryu SE. Crystal structure of DsbDgamma reveals the mechanism of redox potential shift and substrate specificity(1). FEBS Lett 2003;543:164–169. [PubMed: 12753926]

6. Fabianek RA, Hennecke H, Thön-y Meyer L. The active-site cysteines of the periplasmic thioredoxin-like protein CcmG of Escherichia coli are important but not essential for cytochrome c maturation in vivo. J Bacteriol 1998;180:1947–1950. [PubMed: 9537397]
7. Åslund F, Ehn B, Miranda-Vizuete A, Pueyo C, Holmgren A. Two additional glutaredoxins exist in Escherichia coli: glutaredoxin 3 is a hydrogen donor for ribonucleotide reductase in a thioredoxin/glutaredoxin 1 double mutant. Proc Natl Acad Sci U S A 1994;91:9813–9817. [PubMed: 7937896]
8. Miranda-Vizuete A, Damdimopoulos AE, Gustafsson J, Spyrou G. Cloning, expression, and characterization of a novel Escherichia coli thioredoxin. J Biol Chem 1997;272:30841–30847. [PubMed: 9388228]
9. Jordan A, Åslund F, Pontis E, Reichard P, Holmgren A. Characterization of Escherichia coli NrdH. A glutaredoxin-like protein with a thioredoxin-like activity profile. J Biol Chem 1997;272:18044–18050. [PubMed: 9218434]
10. Fernandes AP, Fladvad M, Berndt C, Andresen C, Lillig CH, Neubauer P, Sunnerhagen M, Holmgren A, Vlamis-Gardikas A. A novel monothiol glutaredoxin (Grx4) from Escherichia coli can serve as a substrate for thioredoxin reductase. J Biol Chem 2005;280:24544–24552. [PubMed: 15833738]
11. Bushweller JH, Åslund F, Wüthrich K, Holmgren A. Structural and functional characterization of the mutant Escherichia coli glutaredoxin (C14----S) and its mixed disulfide with glutathione. Biochemistry 1992;31:9288–9293. [PubMed: 1390715]
12. Holmgren A. Glutathione-dependent synthesis of deoxyribonucleotides. Characterization of the enzymatic mechanism of Escherichia coli glutaredoxin. J Biol Chem 1979;254:3672–3678. [PubMed: 34620]
13. Miranda-Vizuete A, Rodriguez-Ariza A, Toribio F, Holmgren A, Lopez-Barea J, Pueyo C. The levels of ribonucleotide reductase, thioredoxin, glutaredoxin 1, and GSH are balanced in Escherichia coli K12. J Biol Chem 1996;271:19099–19103. [PubMed: 8702583]
14. Jordan A, Reichard P. Ribonucleotide reductases. Annu Rev Biochem 1998;67:71–98. [PubMed: 9759483]
15. Ortenberg R, Gon S, Porat A, Beckwith J. Interactions of glutaredoxins, ribonucleotide reductase, and components of the DNA replication system of Escherichia coli. Proc Natl Acad Sci U S A 2004;101:7439–7444. [PubMed: 15123823]
16. Vlamis-Gardikas A, Potamitou A, Zarivach R, Hochman A, Holmgren A. Characterization of Escherichia coli null mutants for glutaredoxin 2. J Biol Chem 2002;277:10861–10868. [PubMed: 11741965]
17. Russel M, Model P, Holmgren A. Thioredoxin or glutaredoxin in Escherichia coli is essential for sulfate reduction but not for deoxyribonucleotide synthesis. J Bacteriol 1990;172:1923–1929. [PubMed: 2180911]
18. Foloppe N, Nilsson L. The glutaredoxin -C-P-Y-C-motif: influence of peripheral residues. Structure 2004;12:289–300. [PubMed: 14962389]
19. Foloppe N, Sagemark J, Nordstrand K, Berndt KD, Nilsson L. Structure, dynamics and electrostatics of the active site of glutaredoxin 3 from Escherichia coli: comparison with functionally related proteins. J Mol Biol 2001;310:449–470. [PubMed: 11428900]
20. Nordstrand K, slund F, Holmgren A, Otting G, Berndt KD. NMR structure of Escherichia coli glutaredoxin 3-glutathione mixed disulfide complex: implications for the enzymatic mechanism. J Mol Biol 1999;286:541–552. [PubMed: 9973569]
21. Nordstrand K, Sandstrom A, Åslund F, Holmgren A, Otting G, Berndt KD. NMR structure of oxidized glutaredoxin 3 from Escherichia coli. J Mol Biol 2000;303:423–432. [PubMed: 11031118]
22. Holmgren A, Åslund F. Glutaredoxin. Methods Enzymol 1995;252:283–292. [PubMed: 7476363]
23. Åslund F, Berndt KD, Holmgren A. Redox potentials of glutaredoxins and other thiol-disulfide oxidoreductases of the thioredoxin superfamily determined by direct protein-protein redox equilibria. J Biol Chem 1997;272:30780–30786. [PubMed: 9388218]
24. Rietsch A, Belin D, Martin N, Beckwith J. An in vivo pathway for disulfide bond isomerization in Escherichia coli. Proc Natl Acad Sci U S A 1996;93:13048–13053. [PubMed: 8917542]
25. Holmgren A. Glutathione-dependent synthesis of deoxyribonucleotides. Purification and characterization of glutaredoxin from Escherichia coli. J Biol Chem 1979;254:3664–3671. [PubMed: 372193]

26. Lillig CH, Prior A, Schwenn JD, Åslund F, Ritz D, Vlamis-Gardikas A, Holmgren A. New thioredoxins and glutaredoxins as electron donors of 3′-phosphoadenylylsulfate reductase. J Biol Chem 1999;274:7695–7698. [PubMed: 10075658]
27. Schriek U, Schwenn JD. Properties of the purified APS-kinase from Escherichia coli and Saccharomyces cerevisiae. Arch Microbiol 1986;145:32–38. [PubMed: 3019265]
28. Lillig CH, Schiffmann S, Berndt C, Berken A, Tischka R, Schwenn JD. Molecular and catalytic properties of Arabidopsis thaliana adenylyl sulfate (APS)-kinase. Arch Biochem Biophys 2001;392:303–310. [PubMed: 11488606]
29. Jorgensen WL, Chandrasekhar J, Madura J, Impey RW, Klein ML. Comparison of Simple Potential Functions for Simulating Liquid water. J Chem Phys 1983;79:926–935.
30. Feller SE, Zhang Y, Pastor RW, Brooks BR. Constant pressure molecular dynamics simulation: The Langevin piston method. J Chem Phys 1995;103:4613–4621.
31. Beck DA, Armen RS, Daggett V. Cutoff size need not strongly influence molecular dynamics results for solvated polypeptides. Biochemistry 2005;44:609–616. [PubMed: 15641786]
32. Norberg J, Nilsson L. On the truncation of long-range electrostatic interactions in DNA. Biophys J 2000;79:1537–1553. [PubMed: 10969015]
33. Ryckaert JP, Berendsen HJC. Numerical integration of the Cartesian equations of motion of a system with constraints: molecular dynamics of n-alkanes. J Comp Phys 1977;23:327–341.G., C.
34. Im W, Beglov D, Roux B. Continuum Solvation Model: computation of electrostatic forces from numerical solutions to the Poisson-Boltzmann equation. Computer Physics Communications 1998;111:59–75.
35. Nina M, Beglov D, Roux B. Atomic radii for continuum electrostatics calculations based on molecular dynamics free energy simulations. Journal of Physical Chemistry B 1997;101:5239–5248.
36. Bashford D, Karplus M. p*K*a's of ionizable groups in proteins: atomic detail from a continuum electrostatic model. Biochemistry 1990;29:10219–10225. [PubMed: 2271649]
37. De Loof H, Nilsson L, Rigler R. Molecular Dynamics Simulation of Galanin in Aqueous and Nonaqueous Solution. J Am Chem Soc 1992;114:4028–4035.
38. Brooks BR, Bruccoleri RE, Olafson BD, States DJ, Swaminathan S, Karplus M. CHARMM: A Program for Macromolecular Energy, Minimization, and Dynamics Calculations. J Comp Chem 1983;4:187–217.
39. MacKerell AD Jr, Bashford D, Belott M, Dunbrack RL, Evanseck JD, Field MJ, Fischer S, Gao J, Guo H, Ha S. All-Atom Empirical Potential for Molecular Modeling and Dynamics Studies of Proteins. J Phys Chem B 1998;102:3586–3616.
40. Mackerell AD Jr. Feig M, Brooks CL 3rd. Extending the treatment of backbone energetics in protein force fields: limitations of gas-phase quantum mechanics in reproducing protein conformational distributions in molecular dynamics simulations. J Comput Chem 2004;25:1400–1415. [PubMed: 15185334]
41. Lee B, Richards FM. The interpretation of protein structures: estimation of static accessibility. J Mol Biol 1971;55:379–400. [PubMed: 5551392]
42. Åberg A, Hahne S, Karlsson M, Larsson Å, Ormö M, Åhgren A, Sjöberg BM. Evidence for two different classes of redox-active cysteines in ribonucleotide reductase of Escherichia coli. J Biol Chem 1989;264:12249–12252. [PubMed: 2663852]
43. Mossner E, Huber-Wünderlich M, Rietsch A, Beckwith J, Glockshuber R, Åslund F. Importance of redox potential for the in vivo function of the cytoplasmic disulfide reductant thioredoxin from Escherichia coli. J Biol Chem 1999;274:25254–25259. [PubMed: 10464247]
44. Åslund F, Nordstrand K, Berndt KD, Nikkola M, Bergman T, Ponstingl H, Jornvall H, Otting G, Holmgren A. Glutaredoxin-3 from Escherichia coli. Amino acid sequence, 1H and 15N NMR assignments, and structural analysis. J Biol Chem 1996;271:6736–6745. [PubMed: 8636094]
45. Gilbert HF. Molecular and cellular aspects of thiol-disulfide exchange. Adv Enzymol Relat Areas Mol Biol 1990;63:69–172. [PubMed: 2407068]
46. Shaked Z, Szajewski RP, Whitesides GM. Rates of thiol-disulfide interchange reactions involving proteins and kinetic measurements of thiol p*K*a values. Biochemistry 1980;19:4156–4166. [PubMed: 6251863]

47. Krantz BA, Melnyk RA, Zhang S, Juris SJ, Lacy DB, Wu Z, Finkelstein A, Collier RJ. A phenylalanine clamp catalyzes protein translocation through the anthrax toxin pore. Science 2005;309:777–781. [PubMed: 16051798]

48. Berardi MJ, Bushweller JH. Binding specificity and mechanistic insight into glutaredoxin-catalyzed protein disulfide reduction. J Mol Biol 1999;292:151–161. [PubMed: 10493864]

49. Krause G, Lundström J, Barea JL, Cuesta CP, Holmgren A. Mimicking the active site of protein disulfide-isomerase by substitution of proline 34 in *Escherichia coli* thioredoxin. J Biol Chem 1991;266:9494–9500. [PubMed: 2033048]

50. Metanis N, Keinan E, Dawson PE. Synthetic seleno-glutaredoxin 3 analogues are highly reducing oxidoreductases with enhanced catalytic efficiency. J Am Chem Soc 2006;128:16684–16691. [PubMed: 17177418]

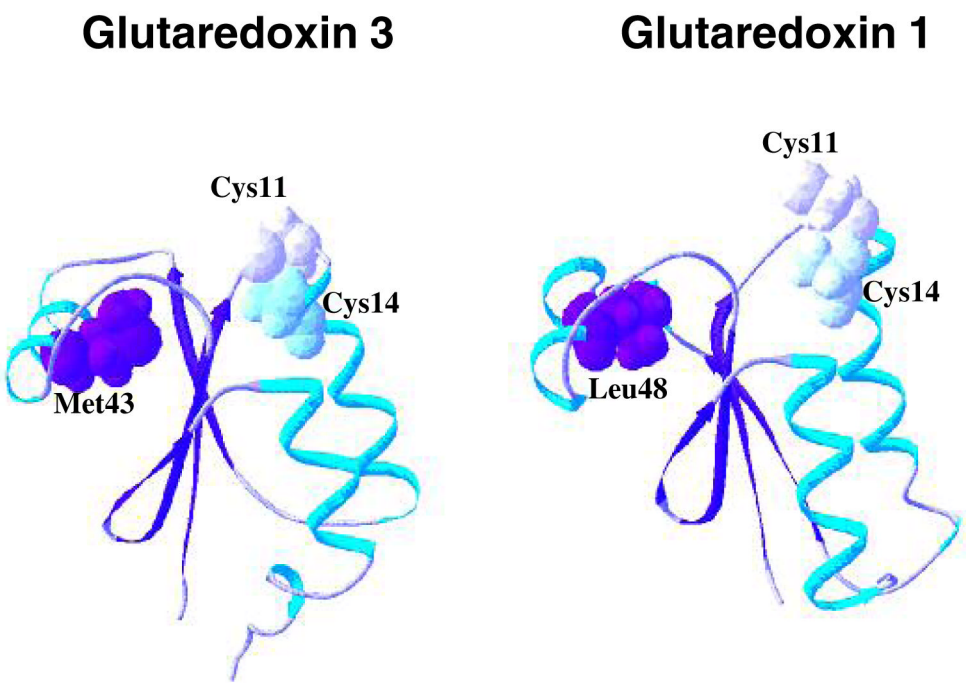

FIGURE 1.

Structures of glutaredoxin 1 and 3. *E. coli* glutaredoxin 1 (Grx1, PDB file 1GRX) (right) and glutaredoxin 3 (Grx3, PDB file 3GRX) (left) consist of the core thioredoxin fold. The two structures are viewed from identical orientation. Secondary structures α-helix and β strands are indicated. The mutated methionine 43 in Grx3 and the equivalent leucine 48 in Grx1, as well as the active-site cysteines (Cys11 and Cys14) located at the beginning of α-helix 1 are presented in a space-filling model. Both structures were determined by using Ser11-X-X-Cys14 mutant proteins.

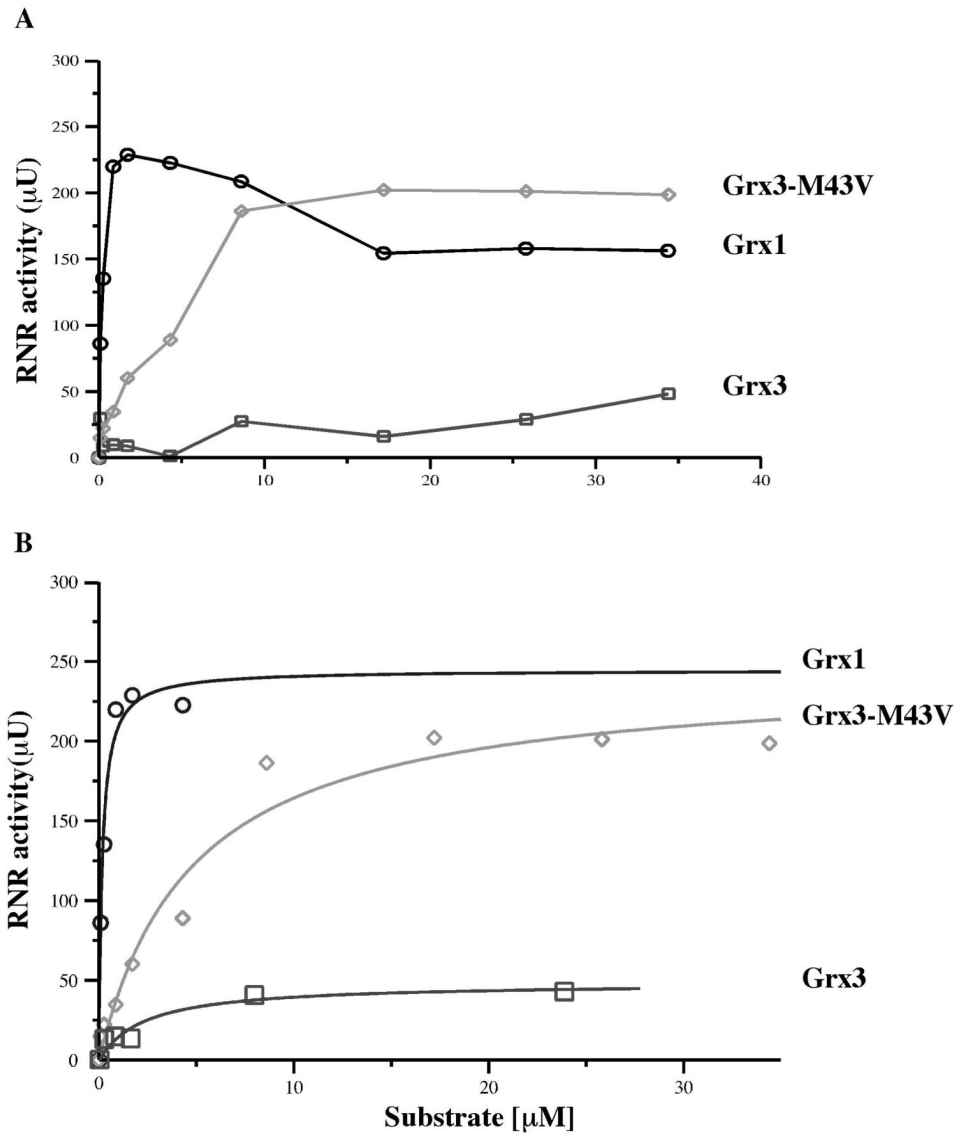

FIGURE 2.

Comparison of Glutaredoxins as hydrogen donors of ribonucleotide reductase. *A*, increasing amounts of glutaredoxin 1 (circle), glutaredoxin 3 (square) or glutaredoxin 3 Met43Val (triangle) were added to standard incubation mixture (materials & methods) supplemented with NADPH regenerating system. The incubation mixture contained 2 μg of *E. coli* ribonucleotide reductase instead of the 6 μg standard. Glutaredoxins were reduced by DTT and desalted prior to addition in the incubation mixture. *B*, non-linear regression analysis curves (Grace-5.1.16™) of ribonucleotide reductase activity for the three glutaredoxins (Panel A) assuming Michaelis-Menten kinetics. The kinetic constants V_{max} and K_m were calculated from the curves using Grace (see Table 3).

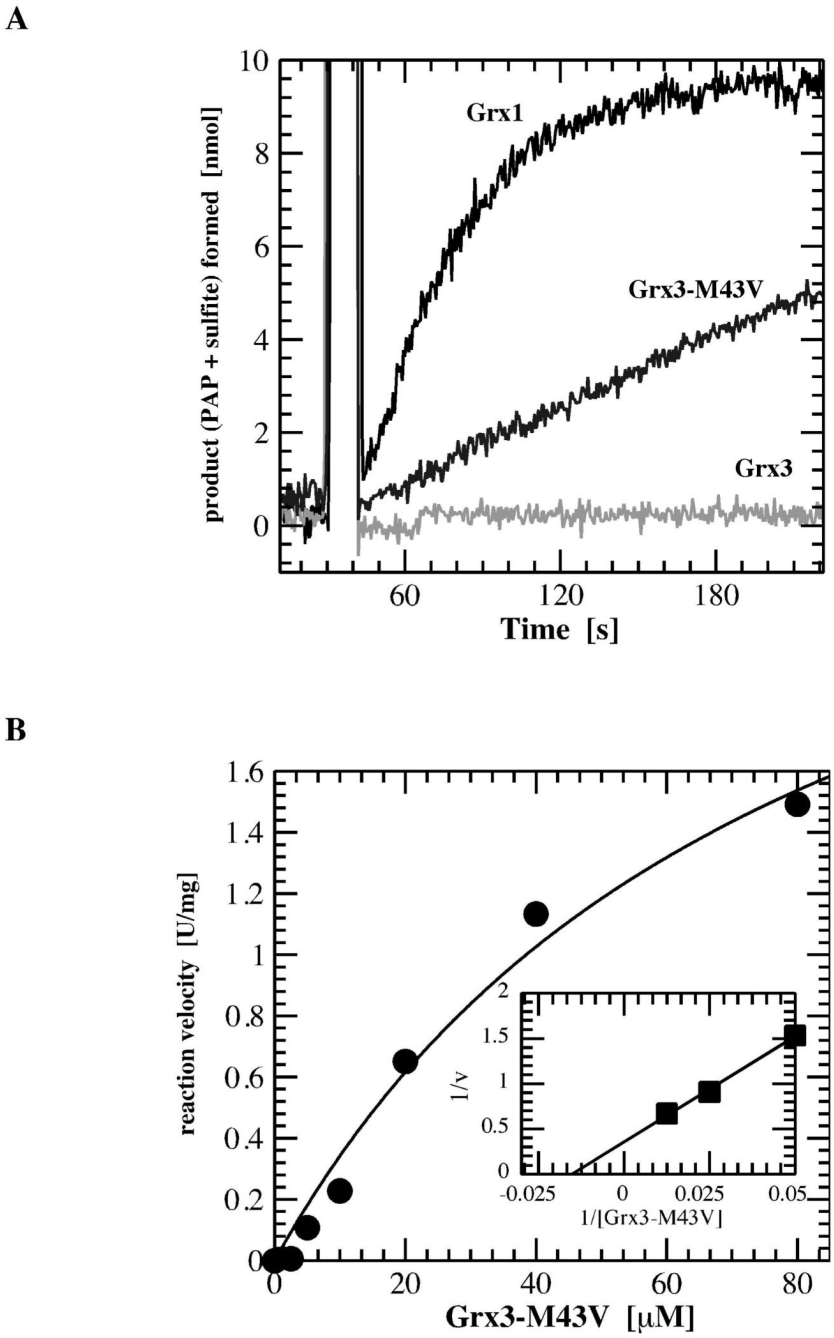

FIGURE 3.

Glutaredoxin 3 Met43Val as hydrogen donor of 3′-phosphoadenylylsulfate (PAPS) reductase. PAPS reductase was measured following NADPH consumption in a coupled assay with yeast glutathione reductase as outlined in the materials and methods. *A*, reduction of 10 nmol PAPS by PAPS reductase (0.5 μg/ml) with glutaredoxin 1, glutaredoxin 3 or glutaredoxin 3 Met43Val as electron donors. *B*, Michaelis-Menten and Lineweaver Burk plots of the initial velocity kinetics of PAPS reductase with glutaredoxin 3 Met43Val as electron donor.

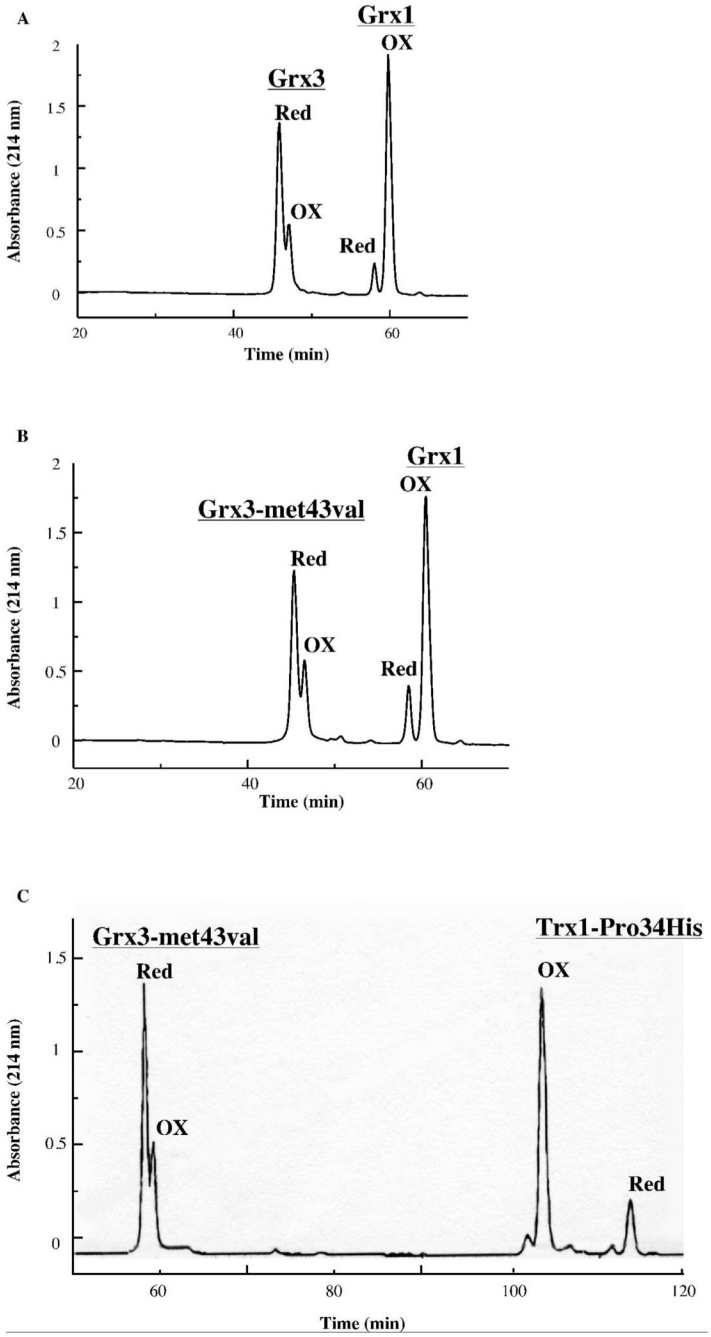

FIGURE 4.

Reverse-phase HPLC chromatograms of redox equilibria between different glutaredoxin and thioredoxin species. Equal concentrations (50 μM) of reduced His_6-tagged *E. coli* glutaredoxin 3 or glutaredoxin 3 M43V were incubated with either oxidized glutaredoxin 1 or thioredoxin 1 P34H in potassium phosphate pH 7.0, 1 mM EDTA buffer for 12 h at 25°C, followed by acid quenching to pH 2.5 before separation of the different species on a C_8 reverse-phase HPLC column (see materials & methods for details). *A*, glutaredoxin 1 and glutaredoxin 3. *B*, glutaredoxin 1 and glutaredoxin 3 M43V. *C*, thioredoxin 1 P34H and glutaredoxin 3 M43V

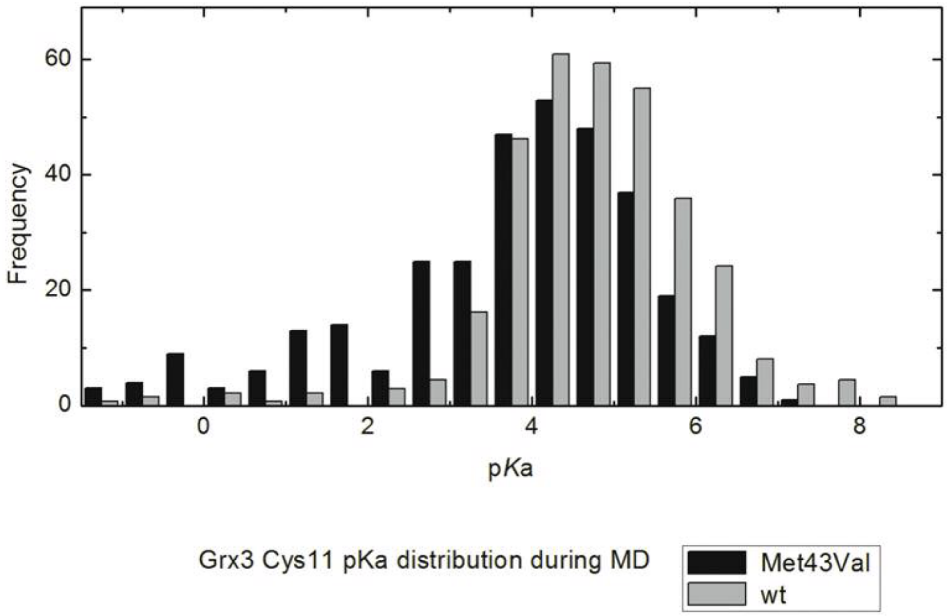

FIGURE 5.

Histogram of Cys11 p*K*a values from simulations. Glutaredoxin 3 Met43Val Cys11 p*K*a values shown in red, and glutaredoxin 3 wild type Cys11 p*K*a values (18) shown in green.

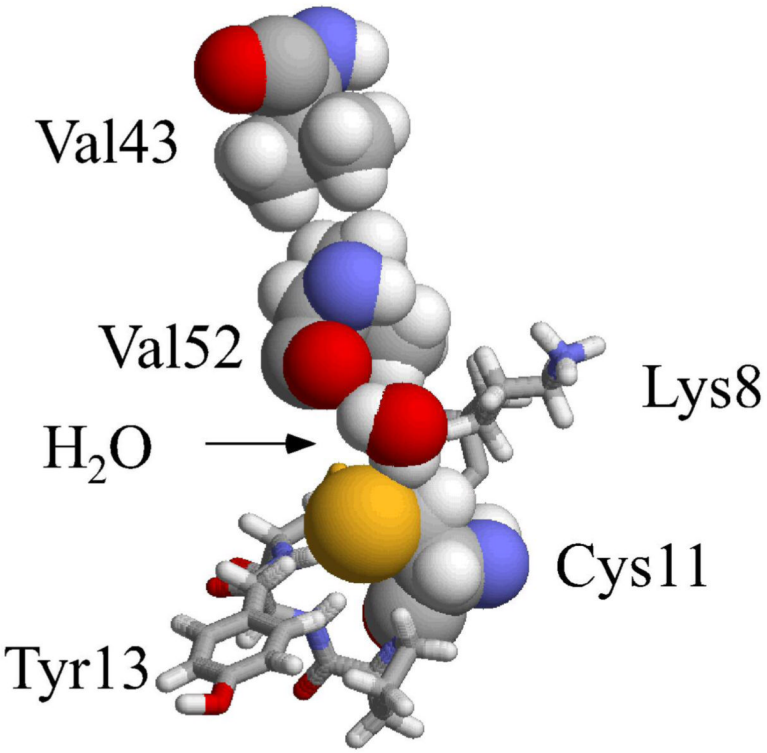

FIGURE 6.

Snapshot from simulation of the glutaredoxin 3 M43V mutant. A water molecule in bridging position between Val52 O and Cys11 S^{γ} is shown. The structure shows Lys8, which at this time is turned away from Cys11, and residue 43 (valine), which makes stable hydrophobic contact with valine 52.

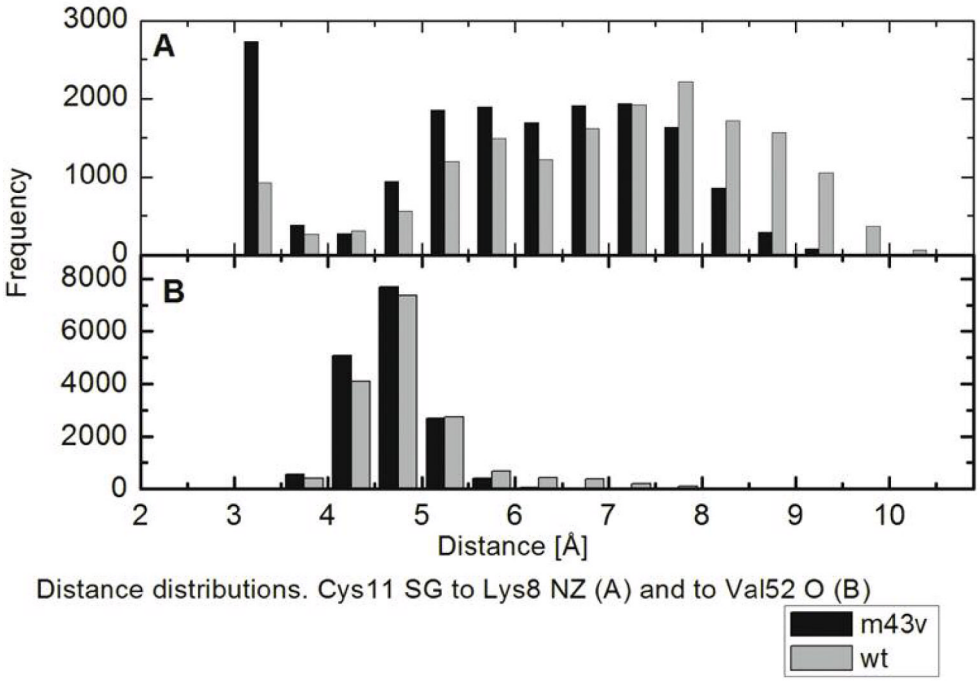

FIGURE 7.

Distance distributions Cys11 S^{γ} to Lys8 N^{ζ} and Val52 O in glutaredoxin 3 Met43Val mutant and wild type simulations. Panel A shows the shorter average distances between Cys11 S^{γ} and Lys8 N^{ζ} as well as the narrower distance distribution in glutaredoxin 3 Met43Val. Panel B shows the slightly shorter average distances between Cys S^{γ} and Val O in glutaredoxin 3 Met43Val.

Table 1

Strains and plasmids used in this work

Strain/plasmids	Relevant genotype or features	Source
Strains		
DH5α	Lab collection	
JM109	*e14-(McrA-) recA1 endA1 gyrA96 thi-1 hsdR17*(rK-mK+) *supE44 relA1 D(lac-proAB)* [F' *traD36 proAB lacIqZDM15]*	(Stratagene)
AM58	JM109, pJAH-*grx-C*	This work
AM60	JM109, pJAH-*grxC*-Met43Val	This work
RO36	DHB4 Δ*trxA* Δ*trxC nrdH*::spc *grxA*::kan, pBAD18-*trxC*	Ref. 15
RO34[a]	RO36 *dnaA*^{sup1}, pBAD18-*trxC*	Ref. 15
Plasmids		
pRO1	pJAH - *grxC* (pACYC184 Ori)	Ref. 15
pQE30	6xHis-tag coding sequence at the 5′ polylinker, phage T5 promoter and pBR322 Ori	Qiagen
pAP14	pJAH - *grxC*-met43val	This work

[a] In RO34, the *dnaA*^{sup1} mutation results in high level expression of ribonucleotide reductase, suppressing the growth defect of the strain on rich media.

Table 2

Kinetic constants of glutaredoxins as electron donors for ribonucleotide reductase[a]

Protein	K_m	V_{max}	Efficiency ($kcat/K_m$)	Correlation coefficient
	$\mu mol\ l^{-1}$	$nmol\ mg^{-1}\ min^{-1}$	$M^{-1}\ s^{-1}$	
Grx1	0.17 ± 0.01	113 ± 9.0	$1.5 \cdot 10^6$	0.99 (n = 6)
Grx3-M43V	4.30 ± 0.8	122 ± 4.0	$6.4 \cdot 10^5$	0.99 (n = 8)
Grx3	3.50 ± 0.95	18 ± 1.5	$1.16 \cdot 10^4$	0.96 (n = 6)

[a] Purified proteins were used. ribonucleotide reductase as a 1:1 mixture of R1 and R2 (2μg). Glutaredoxins were reduced by DTT just before use and then DTT was removed by desalting

Table 3

Kinetic constants of glutaredoxins as electron donors for phosphoadenylyl sulfate reductase[a]

Protein	K_m	V_{max}	Efficiency ($kcat/K_m$)	Correlation coefficient
	$\mu mol\ l^{-1}$	$\mu mol\ mg^{-1}\ min^{-1}$	$M^{-1}\ s^{-1}$	
Grx1	12.7 ± 0.9	4.1 ± 0.3	$1.6 \cdot 10^{5}$	0.99 (n = 3)
Grx3-M43V	79.5± 2.3	3.1 ± 0.3	$1.9 \cdot 10^{4}$	0.99 (n = 3)
Grx3	-	not active	-	-

[a] Purified proteins were used. PAPS reductase was expressed and purified as described (26), PAPS was synthesized enzymatically as described by Schriek and Schwenn (27) using ATP sulfurylase, inorganic pyrophosphatase, pyruvate kinase (Roche) and APS kinase from *Arabidopsis thaliana* purified according to Lillig *et al.* 2001 (28). Glutaredoxins were reduced by DTT just before use and then DTT was removed by desalting.

Table 4

Average number of direct hydrogen bonds from the rest of the protein and water bridges to Cys11 Sγ. Estimated precision ~5%

	Total direct HB	HB to Lys8N$^{\zeta}$	Total water bridges	Cys11 S$^{\gamma}$-w-Lys8N$^{\zeta}$	Cys11 S$^{\gamma}$-w-Val52O
Grx3 wt	2.4	0.06	1.4	0.16	1.1
Grx3 M43V	2.7	0.19	1.7	0.34	1.2

Table 5

Average distance (Å) from Cys11 Sγ. Estimated error of the mean in parenthesis

	Lys8 Nζ	**Val52 O**
Grx3 wt	6.9(0.25)	4.9 (0.1)
Grx3 M43V	5.9 (0.25)	4.7 (0.05)